

Nonequilibrium Edge-State Transport Resolved by Far-Infrared Microscopy

R. Merz, F. Keilmann, R. J. Haug, and K. Ploog

Max-Planck-Institut für Festkörperforschung, 7000 Stuttgart 80, Federal Republic of Germany

(Received 21 August 1992)

Subwavelength focusing of far-infrared light ($\lambda = 392 \mu\text{m}$) is introduced to resolve spatially the photoconductivity of a two-dimensional electron gas. An increased cyclotron resonance amplitude is observed at one of the sample edges which proves that it is at the edge where states with nonequilibrium population can exist.

PACS numbers: 73.50.Pz, 07.60.Pb, 42.79.Gn, 72.20.My

The edge-state model successfully describes the magnetotransport in two-dimensional electron gases (2DEG) [1]. According to this model the current flows in the immediate neighborhood of the sample edges only. In high mobility 2DEGs the coupling between the edge states can be weak enough to allow a nonequilibrium population of edge states [2–4]. Such a nonequilibrium population explains the observation of nonlinear resistance scaling [5] and of nonlocal transport [6]. Photoconductivity measurements under far-infrared radiation showed that in the presence of nonequilibrium transport the cyclotron resonance amplitude is increased, whereas the cyclotron frequency is unchanged [7]. The conclusions in [7] were that—although the mechanism was not identified in detail—the population distribution of the edge states contributes significantly to the photosignal, and that the edge potential cannot be very steep. In these experiments the whole sample was irradiated, and the nonequilibrium was induced by gates, whereas in the present work we use the nonequilibrium which evolves from scattering as discussed below.

Space-resolved measurements of electron transport can in principle give more direct information about the validity of the edge-state model. Experiments with inner contacts [8], however, disturb the potential distribution in the sample, as was shown in experiments [9] using an electro-optic effect for imaging the potential. These experiments showed that under quantum Hall conditions more than 80% of the total Hall voltage drops close to the edges. Klass *et al.* [10] imaged the temperature distribution in a 2DEG sample using the He fountain effect. They identified two hot spots on a Hall bar sample which evidently come from a highly localized current dissipation as the electrons reach a current contact. However, both imaging methods [9,10] require high current and therefore could not resolve spatially the 2DEG transport at the low currents permitted for the edge-state model to be valid.

We have performed spatially resolved far-infrared photoconductivity measurements. The radiation is focused to $\lambda/2$ by transmission through a tapered waveguide with a subwavelength output aperture [Fig. 1(a)] in close proximity of about $\lambda/10$ to the sample. The aperture can be mechanically scanned over the sample surface. The use

of waveguide tapers is well known in microwave technology but has not been applied to enhance the focusing of infrared radiation, which has a practical limit at about 3λ with an $f/3$ lens or mirror system. We use an output aperture diameter not smaller than $\lambda/2$ to avoid total reflection by the cutoff effect. Note, however, that the introduction of a *coaxial* waveguide geometry can eliminate this restriction [11]. Although this technique has allowed us to obtain $\lambda/20$ focus diameters at room temperature [12], problems with mechanical adjustment have prevented its use in the present study.

In our experiment we use a standard AlGaAs/GaAs heterostructure with a carrier concentration $n_s = 2 \times 10^{11} \text{ cm}^{-2}$ and a mobility $\mu = 560000 \text{ cm}^2/\text{Vs}$ at 1.85 K. A Hall bar sample was prepared by photolithography and wet etching, with 0.7 mm channel width and 2.85 mm channel length. As seen in Fig. 1(b) the six potential probes are somewhat receded from the sample sides to avoid an irradiation of the contacts. Metallic top layers outside the channel (not shown) serve to sense by electrical contact the approach of the waveguide tip onto the sample surface. This is routinely done before and after a mechanical scan. The sample is mounted in a variable-temperature exchange gas cryostat inside a superconducting split-coil magnet (Magnex Scientific) on a mechanical x - y translation stage movable from the outside. The magnetic field is oriented in the z direction. A third external screw handle allows one to move the focusing tip in the z direction. The distance from tip to sample is set

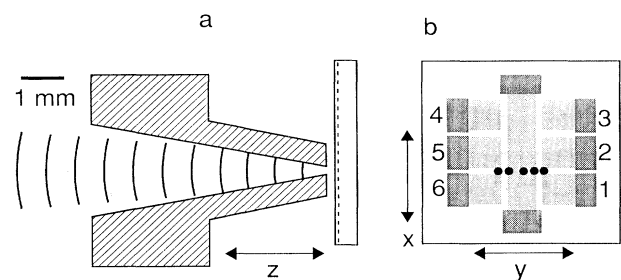


FIG. 1. Scale diagram of (a) focusing metallic waveguide and (b) Hall bar sample; the black dots depict the near-field microscope scan.

to $35 \pm 5 \mu\text{m}$ for the measurement, but is increased to about $100 \mu\text{m}$ for changing the position in the mechanical scan along the y direction. Here the resettability is $\Delta y = \pm 30 \mu\text{m}$. The far-infrared radiation from an optically pumped CH_3OH laser (Edinburgh Instruments) is focused with an $f/6$ lens from outside the cryostat through a 0.2 mm Mylar foil. To obtain a sufficient signal-to-noise ratio in measuring the potential difference between two probes, we alternate the current direction at 555 Hz and use lock-in amplification; note that current reversal flips the side at which net electron current transport occurs, and, thus, our signal represents the potential difference related to the net current.

Nonequilibrium phenomena are known to occur at filling factors $n = 2N + \frac{1}{2}$, where $N = 1, 2, \dots$ in standard Hall bar geometry [13]. For this experiment we chose to work near a filling factor of $n = 4.5$ where the magnetic field is 1.84 T . The nonequilibrium population of edge states becomes manifest by measuring the Shubnikov-de Haas curve [5,13]. The result obtained with our sample [Fig. 2(a)], at a current of $0.3 \mu\text{A}$, agrees with earlier work [14] as it shows that the $n = 4.5$ maximum becomes depressed relative to the maximum at $n = 5.5$, and, thus, a nonequilibrium population builds up along the path of the electrons. The reasons for this behavior are that (i) the electrons in the innermost state are backscattered across the channel and (ii) the innermost state is decoupled from the outer states. The current contacts are assumed to be almost ideal, i.e., the electron-injecting contact equally populates the outgoing states up to the electrochemical potential, and backscattering of the incoming edge states does not occur. In contrast the potential probes are assumed to act as nonideal contacts in the dissipative regime, since the scattering of one edge to the

other across the narrow side arms is very effective and thus obstructs any equilibration action of the contacts [15].

For our experiment with focused far-infrared radiation we chose to scan along a line between the middle and lower potential probes [Fig. 1(b)], since here we can expect to interact with both equilibrium or nonequilibrium edge states depending on which side and in which direction the electrons are chosen to move. The photosignal ΔU is obtained as the change in the potential difference with and without far-infrared radiation on the indicated spot region. At 1.84 T the cyclotron resonance requires a far-infrared wavelength of $\lambda = 393 \mu\text{m}$ for $m^* = 0.0675m_e$. We use a laser at $392 \mu\text{m}$. An unshifted cyclotron resonance is observed. Figure 3(a) shows the signal on resonance with current and magnetic-field directions as indicated in the left part of Fig. 2. The signal amplitude amounts to up to about 10% of the Shubnikov-de Haas voltage. We see that a maximum response is induced by irradiating the right edge. This confirms the earlier indirect conclusion [7] that the photoresponse of a nonequilibrium edge state is enhanced. The photosignal is seen to be reduced when the spot is moved away from the right edge by one nominal spot width of $200 \mu\text{m}$, as to be expected from the edge-state

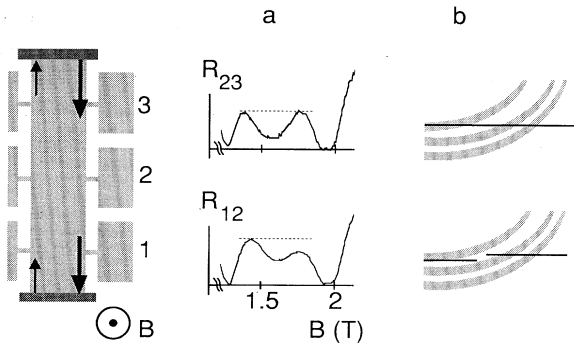


FIG. 2. Partial view of Hall bar illustrating the field orientations (left). The experimental longitudinal resistance R_{12} exhibits, compared to R_{23} , a depressed maximum at filling factor $n = 4.5$ near 1.84 T , relative to the ones at $n = 5.5$ near 1.43 T (a). This depression shows that a nonequilibrium population of edge states evolves as the electrons propagate: As depicted in the energy diagrams (b) three Landau states are bent upwards at the right sample edge, and are populated either equally (upper diagram) or nonequally (lower diagram).

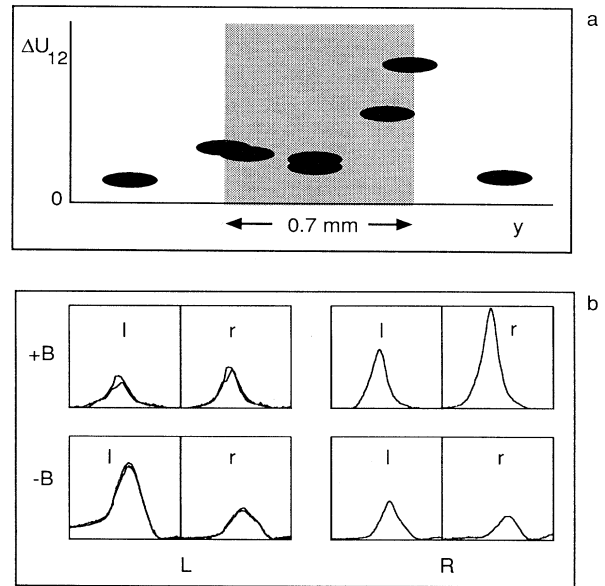


FIG. 3. Photosignal ΔU —i.e., longitudinal potential difference measured between middle and lower probes—induced by focused far-infrared radiation at $\lambda = 392 \mu\text{m}$; (a) right probe pair 1-2, $B = +1.85 \pm 0.03 \text{ T}$, lateral position as indicated; (b) resonance curves for 0.5 T magnetic-field scans ($|B|$ increasing to the right) around $+1.85 \text{ T}$ ($+B$) or -1.85 T ($-B$), with focus on either left edge (L) or right edge (R), and measurement with either left (l) probe pair (5-6) or right (r) probe pair (1-2).

model which confines the edge state to distances well below $1\ \mu\text{m}$ from the edge. The photosignal does not vanish when the focus lies outside the channel, probably because of stray radiation. The spot width drawn in Fig. 3(a) is chosen to be $200\ \mu\text{m}$, but we expect the irradiation width is larger by approximately $50\ \mu\text{m}$ due to diffraction. A slightly enhanced response (compared to the channel center) is seen to occur when the left edge is irradiated. This confirms our expectation that the edge states at some distance from the injecting contact are no longer fully equilibrated.

In Fig. 3(b) we display the cyclotron resonance traces of the photosignal for focus positions just on either the left or right edge, with different choices of the magnetic field direction (which determines on which side the net electron current is flowing), and with measurement on opposite probe pairs. Again the results confirm our overall interpretation: enhanced photoresponse on the right edge is only seen with $(+B)$ magnetic field and using right probes, and, *vice versa*, enhanced photoresponse on the left edge is only seen with $(-B)$ magnetic field and using left probes.

The enhanced photoresponse of nonequilibrium states can be explained as in Ref. [7] by a photon-induced enhancement of the inter-edge-state scattering rate; this leads to enhanced electron transfer from the outer to the innermost edge state from where efficient backscattering across the channel takes place. Further experiments were performed with a different sample which did not exhibit a depression of the $n=4.5$ Shubnikov-de Haas maximum, which means that nonequilibrium transport at the edges was absent. Quite as expected for an equilibrium edge-state population the photosignal did not show any dependence on the spatial position of the laser focus within the sample.

In conclusion, we have demonstrated a method to focus infrared light to a spot smaller than the wavelength, and to mechanically scan this focus in a cryomagnet. In applying this method to study photoconductivity of a 2DEG in the quantum Hall regime, we observe a large photosignal only when the focus is on the particular sample edge where the edge-state population is known to be not in equilibrium. This result directly manifests the central prediction of the edge-state model that 2D transport in

fact occurs at the edges.

We thank K. W. Kussmaul for expert mechanical construction, as well as A. D. Wieck, F. Kuchar, and M. Meisels for discussions. Thanks go also to F. Schartner, S. Tippmann, and M. Wurster for sample preparation.

-
- [1] For example, M. Büttiker, in *Festkörperprobleme*, edited by U. Rössler (Vieweg, Braunschweig, 1990), Vol. 30, pp. 41–52, and references therein.
 - [2] B. J. van Wees, E. M. M. Willems, C. J. P. M. Harmans, C. W. J. Beenakker, H. van Houten, J. G. Williamson, C. T. Foxon, and J. J. Harris, *Phys. Rev. Lett.* **62**, 1181 (1989).
 - [3] B. W. Alphenaar, P. L. McEuen, R. G. Wheeler, and R. N. Sacks, *Phys. Rev. Lett.* **64**, 677 (1990); G. Müller, D. Weiss, S. Koch, K. von Klitzing, H. Nickel, W. Schlapp, and R. Lösch, *Phys. Rev. B* **42**, 7633 (1990).
 - [4] S. Komiyama, H. Hirai, S. Sasa, and S. Hiyamizu, *Phys. Rev. B* **40**, 12566 (1989).
 - [5] R. J. Haug and K. v. Klitzing, *Europhys. Lett.* **10**, 489 (1989).
 - [6] P. L. McEuen, A. Szafer, C. A. Richer, B. W. Alphenaar, J. K. Jain, A. D. Stone, R. G. Wheeler, and R. N. Sacks, *Phys. Rev. Lett.* **64**, 2062 (1990).
 - [7] E. Diessel, G. Müller, D. Weiss, K. von Klitzing, K. Ploog, H. Nickel, W. Schlapp, and R. Lösch, *Appl. Phys. Lett.* **58**, 2231 (1991).
 - [8] G. Ebert, K. von Klitzing, and G. Weimann, *J. Phys. C* **18**, L257 (1985); H. Z. Zheng, D. C. Tsui, and A. M. Chang, *Phys. Rev. B* **32**, 5506 (1985); K. Sichel, H. H. Sample, and J. P. Salerno, *Phys. Rev. B* **32**, 6975 (1985).
 - [9] P. F. Fontein, J. A. Kleinen, P. Hendriks, F. A. P. Blom, J. H. Wolter, H. G. M. Lochs, F. A. J. M. Driessen, L. J. Giling, and C. W. J. Beenakker, *Phys. Rev. B* **43**, 12090 (1991).
 - [10] U. Klass, W. Dietsche, K. von Klitzing, and K. Ploog, *Z. Phys. B* **82**, 351 (1991).
 - [11] F. Keilmann, U.S. Patent No. 4994818, 1991.
 - [12] R. Merz, doctoral thesis, Universität Stuttgart, 1992 (unpublished).
 - [13] B. J. van Wees, E. M. M. Willems, L. P. Kouwenhoven, C. J. P. M. Harmans, J. G. Williamson, C. T. Foxon, and J. J. Harris, *Phys. Rev. B* **39**, 8066 (1989).
 - [14] R. J. Haug, K. von Klitzing, K. Ploog, and P. Streda, *Surf. Sci.* **229**, 229 (1990).
 - [15] R. J. Haug, *Semicond. Sci. Technol.* (to be published).